provided by CiteSeerX

M. Toren
Y. Zvirin
Y. Winograd[1]

Faculty of Mechanical Engineering,
Technion—Israel Institute of Technology,
Haifa, Israel

Melting and Evaporation Phenomena During Electrical Erosion

A modeling method is presented for the evaluation of the eroded crater during electrical discharge machining. The method is based on the propagation of the melting crater when other effects such as evaporation can take place. Calculations are performed for a point heat source on the surface of copper and steel electrodes. An experimental technique for the measurement of the amount of eroded material is described: the method consists of extraction of the metal from the dielectric fluid by chemical reactions and measurement of the resulting color intensity.

1 Introduction

Electrical discharge machining (EDM) of metals has become an established method for machining, especially for complicated geometries and high accuracy. The practical techniques of EDM have developed considerably in recent years. However, in spite of the progress made in the theory of EDM, many aspects of the process are still unexplained. The process of the discharge between two electrodes (tool and workpiece) immersed in a dielectric fluid is very complicated and involves numerous phenomena, e.g., heat conduction and phase changes (melting, evaporation, ionization, excitation) of the electrodes and the dielectric fluid, electrical forces, formation and collapse of gas bubbles and energy distribution in the discharge channel. Several very simplified mathematical models for the erosion mechanisms have been suggested, but a generally accepted theory does not yet exist.

Electrical forces exerted by the electric field between the electrodes can account for the erosion only for very short pulses—up to 10^{-6} s, [1–4].[2] For longer pulses, the basic mechanism for metal removal is that of melting and evaporation [5–14]. The discharge channel is the energy source and the amount of eroded material is determined by the isotherm of the melting temperature. The mathematical models suggested [5–14] for this mechanism treat the melting process by modification of the specific heat of the material and not by sinks of latent heat. Evaporation is either neglected or it is assumed that the surface temperature does not exceed the evaporation temperature. While these assumptions can be justified for approximate calculations, a more accurate approach must take into account the latent heat of evaporation, which is much larger than that of melting. Moreover, other phenomena such as ionization and excitation of the evaporated material can occur, and the existing mathematical models cannot describe them.

Problems of heat transfer with a change of phase are also encountered in other fields, such as solidification of castings, design of shields for re-entry vehicles on the basis of aerodynamic ablation, freezing of foodstuffs and sinks for energy storage. Boley [15] and Muehlbauer and Sunderland [16] presented a thorough review of the literature published until 1963, which was limited to a single change of phase depending on a single space variable. Since 1963 several authors treated two- and three-dimensional problems, but only a single change of phase. Several of these works are mentioned by Budhia and Kreith [17], who solved the problem of melting in a wedge.

Sikarskie and Boley [18] solved the problem of heat transfer with melting caused by a heat source which varies spatially along the boundary surface. They have also suggested a method for treating the initial propagation of the melting front, based on the assumption that the problem can be regarded as one-dimensional during the initial stages. Pedroso and Domoto [19] suggested a perturbation method for solidification problems. They simplified the problem by transforming the variables such that the position of the solidification front replaces time. Lazaridis [20] presented an implicit numerical solution for the temperature field and the position of the interface for a multidimensional solidification. He treated, again, only a single phase-change.

[1] This paper is dedicated to the memory of Prof. Y. Winograd who was killed in action during the Yom-Kippur War, October 1973, while defending his country.

[2] Numbers in brackets designate References at end of paper.

Contributed by the Heat Transfer Division for publication in the JOURNAL OF HEAT TRANSFER. Manuscript received by the Heat Transfer Division September 17, 1974. Paper No. 76-HT-J.

 Copyright © 1975 by ASME

Downloaded From: https://heattransfer.asmedigitalcollection.asme.org on 06/29/2019 Terms of Use: http://www.asme.org/about-asme/terms-of-use

This present work is apparently the first attempt to develop a method for treating a heat transfer problem with multiple phase changes. The method can serve as a first approximation for evaluating the propagation of the melting crater during electrical discharge machining.

The model is applied here to calculate numerically the melting isotherm resulting from a single spark of a point source on the electrode surface when melting and evaporation take place. These phenomena are first included accurately, by sinks of latent heats distributed on the melting and evaporation isotherms (Section 2). In Section 3 an approximate method is developed in which the sinks due to melting and evaporation are "transferred" to the site of the point source. The magnitudes of these sinks remain as in the exact model, i.e., the heats required to melt and evaporate the propagating melting and evaporation shells. The results for copper and steel electrodes show that the approximate model is sufficiently accurate for practical calculations. This method is clearly simpler than the exact one and enables a considerable reduction of numerical computation and thus of computer time.

In order to develop these simple models which represent the complicated process of the discharge, several assumptions need be made. The first one is that of spherical symmetry. It is well known, c.f., Soneys and Van Dyck [14] and Greene and Guerrero-Alvarez [21], that the crater formed by a single spark is a symmetrical segment, which tends to a half-sphere with increasing pulse duration. This is explained by the following reasons: the diameter of the discharge channel is much smaller than that of the workpiece electrode, heat conduction into the dielectric fluid is negligible compared with that in the metallic electrode, and convection in the vapor phase is not important until the collapse of the bubble which contains the vapor. It is believed, e.g., Zolotych [8] and Crookall and Heuvelman [22], that some evaporation of the dielectric fluid takes place at the beginning of the discharge. The electric arc is then established in this gap, while more vapor, mainly from the electrodes, is accumulated in a bubble. The bubble collapses only after termination of the discharge (for pulse durations up to 1000 μs, investigated here). Convection in the vapor phase can be important only then; it is neglected in the present work. This assumption is further justified by the results of Greene and Guerrero-Alvarez [21]. They compared machining in a dielectric fluid and in a gas. In the former case, a single crater is created while in the latter, secondary craters are formed around the central main crater. This shows that the dielectric fluid prevents the spreading of the energy and hinders convection.

A further assumption is that the properties are constant and equal in all three phases. In most of the reported works on melting or solidification the problem of the properties in the different phases is avoided. For example, Sikarskie and Boley [18] considered instantaneous removal of the melted material and heating applied to the melting front. The same authors, and also Budhia and Kreith [17], solved problems in which the whole liquid phase is at the melting temperature. In order to accommodate the change in the properties between the phases, sophisticated and complicated numerical methods must be used, e.g., Lazaridis [20]. In the existing models for electrical discharge machining, evaporation and melting are not included directly, as mentioned in the foregoing. For the former, it was assumed that the surface temperature does not rise above that of evaporation; for the latter, constant and equal properties are assumed for the solid and liquid phases, and the specific heat capacity was modified by the latent heat to account for melting, Snoeys and Van Dyck [14]. Cobine and Burger [23] even assumed that all the energy supplied is absorbed by evaporation.

Observation of the behavior of the relevant physical properties for metals, c.f., Smithells [24], shows that they do not change drastically at the melting point. Some properties vary continuously through this point while the discontinuous change in other properties is small. Since the variations of the properties between the solid and liquid phases are quite moderate and due to the fact that the crater is tiny, the assumption of constant properties seems reasonable as a first approximation.

The properties of the vapor phase still remain a difficulty and a limitation of the model. However, since the electric current penetrates through the vapor phase, most of the heat is applied at the liquid-vapor front so that heating of the vapor and conduction in it are not important. The dominant effects are melting and evaporation, and only when the temperatures are much higher, ionization and excitation in the gas phase become significant. Moreover, the thermal resistance of the vapor phase is also compensated for by solid particles in the crater which are torn from the electrode surface during the first stages of the discharge, c.f., Zolotych [8].

The experimental part of the work included measurements of the quantities removed from the electrodes during single discharges. One of the main problems of measuring the amount of material eroded during a single spark is that this amount is very small. One method is based on measurement of the dimensions of the crater [6, 12, 13], but the shape of the crater becomes irregular with increasing pulse duration. Another method is based on averaging the weight loss of the workpiece resulting from many sparks [25–26]. In this way, however, every spark has a new configuration. Determination of the erosion by radioactive tracers [27] gives reasonable results but was found to be inconvenient.

The experimental method reported here (Section 4) for measurement of the amount of eroded metals consists of chemical extraction of the metal from the dielectric fluid and determination of its quantity by the intensity of colored solutions in a spectro-photometer.

The experimental results for copper and steel electrodes are compared with those of the theoretical model. Good agreement is found for intermediate pulse duration; for longer and shorter pulses the theory can provide orders of magnitudes of material removal. It is thus concluded that the simple model can serve as a first approximation in spite of the assumptions and simplifications which were being made.

2 Propagation of the Melting and Evaporation Surfaces

The basic mechanism of metal removal during EDM is based on melting and evaporation. The discharge channel is the heat source, assumed here to be constant and concentrated at a point on the surface of the electrode. The crater of eroded material is determined by the isotherm of the melting temperature, see Fig. 1.

Nomenclature

c = special heat
k = heat conductivity
ℓ = length scale
L = latent heat
M = melting parameter
q_M, q_V = heat sinks due to latent heats of melting and evaporation, respectively
Q = point heat source
r = radius, dimensionless
R = radius
t = time
t^* = time scale
T = temperature
V = evaporation parameter
w_M, w_V = temperatures due to heat sinks of melting and evaporation, dimensionless
α = heat diffusivity
$\delta()$ = Dirac delta function
θ = temperature, dimensionless
τ = time, dimensionless
ρ = density
ψ = temperature due to a point heat source, dimensionless

Subscripts:

M = melting
V = evaporation
0 = initial time

Downloaded From: https://heattransfer.asmedigitalcollection.asme.org on 06/29/2019 Terms of Use: http://www.asme.org/about-asme/terms-of-use

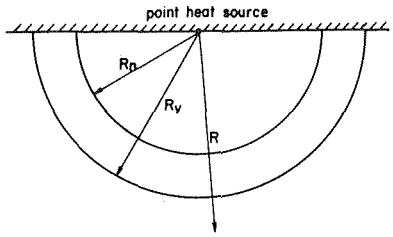

Fig. 1 The melting crater

As mentioned in the foregoing, it is assumed that the physical properties are constant and equal for the phases. The temperature field in the metal can be described then by the following Fourier equation:

$$\rho c \frac{\partial T}{\partial t} - k\nabla^2 T = Q\delta(\vec{R}) - q_M(\vec{R}_M; t) - q_V(\vec{R}_V; t) \tag{1}$$

where Q is the intensity of the heat source and q_M and q_V are the instantaneous heat sinks due to melting and evaporation taking place at $\vec{R}_M$ and $\vec{R}_V$:

$$q_M(\vec{R}_M; t) = \frac{4}{3}\pi\rho L_M \frac{d}{dt} R_M{}^3 \tag{2a}$$

$$q_V(\vec{R}_V; t) = \frac{4}{3}\pi\rho L_V \frac{d}{dt} R_V{}^3 \tag{2b}$$

Other phenomena like ionization and excitation can be described by adding appropriate terms on the right-hand side of equation (1).

The initial condition is taken as a uniform temperature T_0, just before application of the source:

$$T = T_0 \text{ at } t = 0 \tag{3}$$

It is assumed that the heat loss from the surface of the electrode is negligible (see Fig. 1); thus, because of symmetry, the problem reduces to a spherical one-dimensional one. The other boundary condition is:

$$T \text{ finite as } R \to \infty \tag{4}$$

which states that the dimensions of the crater are much smaller compared with the electrode.

Equation (1) for the temperature is linear, therefore, the solution can be composed of three terms, written in the following dimensionless form (cf., Carslaw and Jaeger [28], p. 293):

$$\theta(r, \tau) = \psi(r, \tau) - Mw_M(r, \tau; r_M) - Vw_V(r, \tau; r_V) \tag{5}$$

where the functions ψ, w_M, and w_V denote the temperature fields resulting from a point source at $r = 0$ and from heat sinks (due to melting and evaporation) distributed on the propagating fronts $r_M(\tau)$ and $r_V(\tau)$, respectively.

The dimensionless variables θ, r, and τ are defined by:

$$\theta = \frac{T - T_0}{T_M - T_0};\quad r = \frac{R}{\ell};\quad \tau = \frac{t}{t^*} \tag{6}$$

where the length and time scales are:

$$\ell = \frac{Q}{4\pi k(T_M - T_0)};\quad t^* = \frac{\ell^2}{4\alpha} \tag{7}$$

It is noted that the length scale is chosen as the radius of the melting crater at the steady state.

The dimensionless parameters M and V which represent the relative importance of melting and evaporation, are defined as follows:

$$M = \frac{4}{3\pi^{1/2}} \frac{L_M}{c(T_M - T_0)};\quad V = \frac{4}{3\pi^{1/2}} \frac{L_V}{c(T_M - T_0)} \tag{8}$$

The functions ψ, w_M, and w_V are given by Carslaw and Jaeger [28]:

$$\psi(r, \tau) = \frac{1}{r}\operatorname{erfc}\frac{r}{\sqrt{\tau}} \tag{9}$$

$$w_M(r, \tau; r_M) = \int_0^\tau \frac{1/3\, d/d\tau' \, r_M{}^3}{4\pi r_M(\tau')} \frac{d\tau'}{(\tau - \tau')^{1/2}} \left\{ e^{-[r - r_M(\tau')]^2/(\tau - \tau')} + \right.$$

$$\left. - e^{-[r + r_M(\tau')]^2/(\tau - \tau')} \right\} \tag{10}$$

and a similar expression for w_V, obtained by replacing the subscript M by V in equation (10).

From (5), (9), and (10) it is seen that the temperature at any time τ depends on the history of the melting and evaporation propagation from the start ($\tau = 0$) to this time τ. In order to evaluate the increase with time of the radii r_M and r_V, it is necessary to solve two equations which follow from (5) with $\theta = \theta_M$ and $\theta = \theta_V$:

$$\theta_M - [\psi(r_M, \tau) - Mw_M(r_M, \tau; r_M) - Vw_V(r_M, \tau; r_V)] = 0 \tag{11a}$$

$$\theta_V - [\psi(r_V, \tau) - Mw_M(r_V, \tau; r_M) - Vw_V(r_V, \tau; r_V)] = 0 \tag{11b}$$

Equations (11) were solved numerically for $r_M(\tau)$ and $r_V(\tau)$. The computer program performs the numerical quadrature of the integrals which appear in (10), when $r_M(\tau')$ and $r_V(\tau')$ for $0 < \tau' < \tau$ are known from the previous steps and $r_M(0) = r_V(0) = 0$. The system of two simultaneous nonlinear equations (11) for $r_M(\tau)$ and $r_V(\tau)$ is solved by iteratively minimizing the sum of the squared left hand sides of equations (11a) and (11b). The method of solution can be applied to any metal; the solution in the dimensionless form depends on the metal properties (via M and V), thus, a complete universal solution cannot be obtained.

Results for the propagation of the melting and evaporation fronts for copper and steel are shown in Figs. 2 and 3. Obviously, R_M and R_V tend asymptotically to constant values as time becomes very large. Then a steady state is reached where all the heat from the source is conducted into the solid.

The asymptotic radius of the melting isotherm for copper is smaller than that of steel, because the product kT_M is larger for copper (see equations (6), (7), and (9)). For short times, the dominant phenomenon is that of evaporation which requires the largest part of the energy. The latent heat of evaporation is bigger for steel than for copper; therefore, the melting radius of steel is smaller for short times. Moreover, this phenomenon also causes

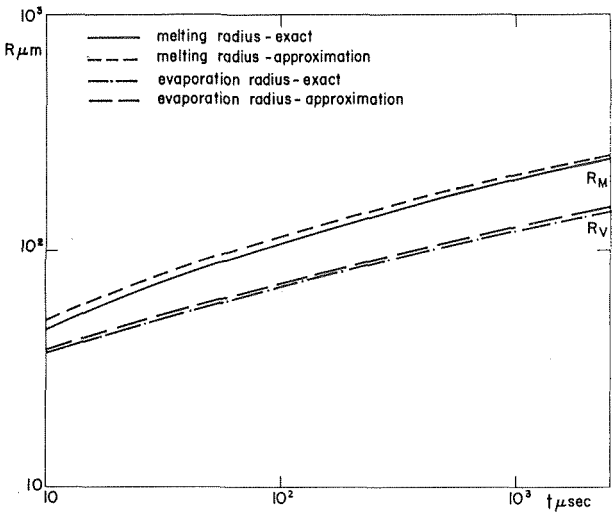

Fig. 2 Propagation of melting and evaporation radii r_M and r_V with time for copper—continuous point source of 2000 W

Downloaded From: https://heattransfer.asmedigitalcollection.asme.org on 06/29/2019 Terms of Use: http://www.asme.org/about-asme/terms-of-use

the melting and evaporation radii of steel to be closer to one another than for copper (see Fig. 2 and 3).

3 Approximate Method for Calculation of Metal Removal

The method described in the foregoing for calculation of the propagation of the melting isotherm is an exact method. Its application to the problem of a point source requires a considerable amount of numerical work and of computer time. For more complex problems the exact method may become cumbersome and a significant increase of numerical computation will be needed. Therefore, an approximate model is suggested, which simplifies the evaluation of the melting crater while taking into account all the phenomena involved. The approximation is made by "transferring" the sinks of melting and evaporation to the site of the point source. The magnitudes q_M and q_V of these sinks remain, however, as in the exact model, equations (2*a*) and (2*b*). Other effects such as ionization and excitation can be included in the model by the addition of similar terms.

The temperature field is, again, expressed by equation (5), but in the approximate model w_M is the temperature field resulting from a time dependent heat source at the origin [28]:

$$w_M = \int_0^\tau \frac{d}{dt} r_M{}^3 \frac{1}{(\tau - \tau')^{3/2}} e^{-r^2/(\tau-\tau')} \qquad (12)$$

and similarly for w_V.

The results of the approximate model for copper and steel are shown in Figs. 2 and 3 and compared with those of the exact method. It can be seen that the approximations are very good, justifying the adoption of this model.

The total erosion of the electrode is found by calculating the volume of the melting crater; in the case of a point source the crater is a half-sphere. The total mass of copper and steel removed by melting and evaporation are plotted in Figs. 4 and 5 versus pulse duration for several source powers. The results show that during short pulses copper is eroded more than steel (for the same power supply) and vice versa for long pulses. The reason is that at the beginning of the pulse melting and evaporation consume most of the energy. As time increases, a steady state is approached where melting and evaporation tend to stop and the energy is conducted into the solid. The latent heats of steel are higher than those of copper; therefore melting and evaporation are more rapid in the latter metal. Since the heat conductivity (or rather kT_M) of copper is higher than for steel, the asymptotic eroded crater is smaller in copper, as explained in the foregoing. These conclusions are also confirmed by the experimental results, see Fig. 6.

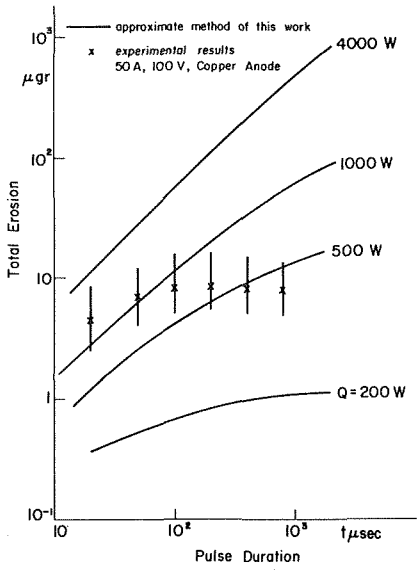

Fig. 4 Total mass of copper eroded by a point source, as a function of the pulse duration

4 Experimental Technique and Results

A single spark is discharged between two electrodes in a cup filled with a dielectric fluid (kerosene), see Fig. 7. The eroded metal is extracted from the dielectric fluid by chemical reaction and the amount is measured by the intensity of colored solutions in a spectro-photometer.

The experimental rig is described in detail in a previous article [27]. The upper electrode is a rod (diameter 6 mm) tapered to a cone and the lower one is a disk (diameter 12 mm, thickness 3 mm). The gap spacing between them is 10 μm and is measured by a micrometer (accuracy 1 μm). The point of contact between the electrodes is determined by the closing of an electrical circuit through an ohm-meter. The pulse generator is capable of producing a rectangular pulse of duration above 20 μs. Experiments were

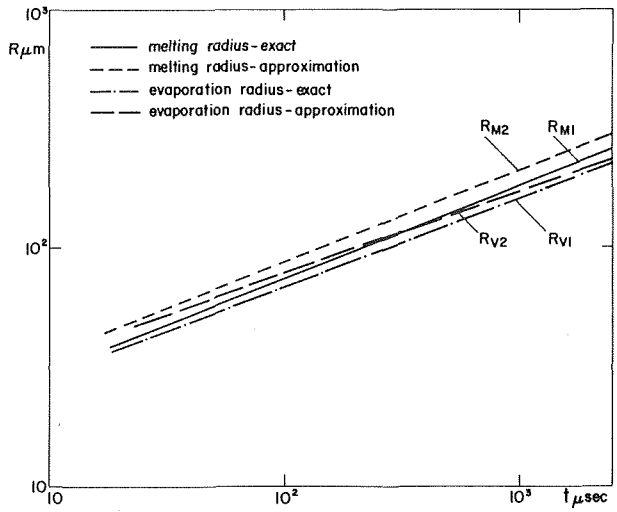

Fig. 3 Propagation of the melting and evaporation radii r_M and r_V with time for steel—continuous point source of 2000 W

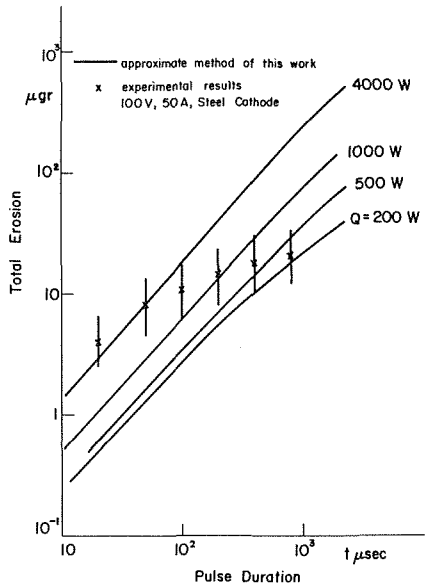

Fig. 5 Total mass of steel eroded by a point source as a function of the pulse duration

Downloaded From: https://heattransfer.asmedigitalcollection.asme.org on 06/29/2019 Terms of Use: http://www.asme.org/about-asme/terms-of-use

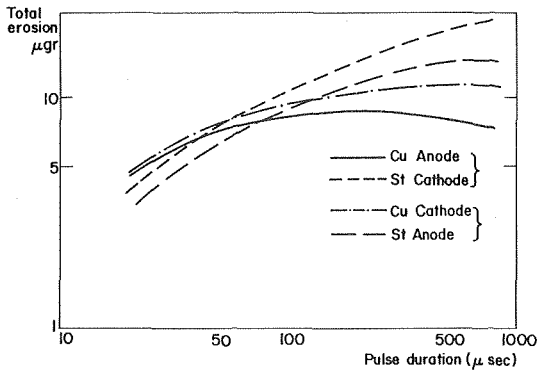

Fig. 6 Total erosion of copper and steel electrodes: 100 V, 50 A

carried out with pulses of 20–1000 μs, pulse voltage of 100 V and current of 50 A. The shape of the pulse is observed in a Tektronix memory oscilloscope. The pulse duration is measured from the moment of breakdown, after the "ignition delay."

The sparks reported here were made between copper and steel. Experiments were carried out first with a conical copper electrode and then with a conical steel electrode. Several experiments were conducted for every pulse duration (20, 50, 100, 200, 400, and 800 μs) and then the polarity was changed for the same configuration.

After each pulse a solution of 10 cm^3 HNO_3 (1:3) is added to the kerosene and dissolves all the eroded metal. The solution is separated and a biquinoline solution is added and reacts with the copper to form a pink colored solution. This solution is separated and the color intensity is measured in the Spectronic 20 spectro-photometer. The amount of copper is determined from a calibration curve. Now, to the other phase which contains the steel, more HNO_3 is added (to pH = 1) and 10cm^3 of 1.5 potassium-thio-cyanate. The latter reacts with the steel and forms a yellow solution. The color intensity is measured, again in the spectro-photometer, and the amount of steel is also determined from a calibration curve.

The experimental results for total erosion of the disk-shaped electrode during a single spark are shown in Fig. 6. It is seen that copper is eroded more than steel at short times (short pulses) and steel is eroded more than copper for long times (long pulse durations), in agreement with the theoretical predictions. Fig. 6 also shows the effect of polarity: erosion is higher when the disk-shaped electrode (the workpiece) is the cathode. This known phenomenon cannot be explained by the melting and evaporation mechanism.

Figs. 4 and 5 include a comparison between the experimental and theoretical results for copper and steel. For each pulse duration, several measurements of single sparks were conducted. The experimental results presented in Figs. 4 and 5 include the averages of these measurements together with the range of variation for each case. The spectro-photometer used for measuring the amounts of the removed metals, is very sensitive. The error involved in measuring amounts of steel and copper did not exceed 0.5 μgr, in the range of the experiments discussed here. It is noted that when the chemical procedure is complicated and takes time, the color of the solution can change if it is exposed to the light. For steel and copper, however, the chemical method is simple and takes only minutes, so there was no such problem. The main reason for the variation in the experimental results is probably the complicated nature of the process of EDM. For example, tiny particles are torn from the electrode surface by electric forces at the beginning of the pulse, e.g., Williams [1–4]. The size and location of such particles depend on the metallurgical condition of the electrode surfaces; since these cannot be exactly reproduced, one cannot expect all the discharges to be exactly the same.

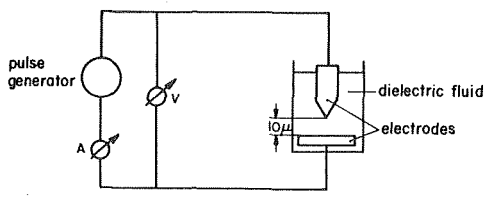

Fig. 7 Schematic arrangement of the EDM circuit

As mentioned in the foregoing, the actual process occurring during the discharge is very complicated. The analytical model presented in this work is a simplified procedure to describe the dominant phenomena of the process, namely melting and evaporation. A more exact model should take into account the energy distribution in the channel, reactions and phase changes in the dielectric fluid, electrical forces, convection in the gas phase, and more complex geometries. Therefore, the theoretical results of this simplified model can hardly be expected to match the experimental findings exactly.

However, it can be seen from Figs. 4 and 5 that for intermediate pulse durations this simple model yields reasonable estimates of total erosion. The agreement between the results indicates that evaporation and melting of the metals are indeed the dominant effects for intermediate pulse durations. For very short pulses electrical forces are considered to be more important [1–4].

For long pulses, a steady state is approached whereby evaporation and melting tend to stop; in this range the experimental results show that the asymptotic constant value of eroded mass is much lower and is reached much sooner than the theoretical predictions. This can be explained by several reasons: (*a*) the discharge channel has a finite width causing a heat source distributed on a finite area rather than a point source; (*b*) ionization and excitation of the evaporated metal and the dielectric fluid take place, requiring energy thus decreasing the energy available for melting; (*c*) a certain part of the eroded material fuses back in the crater after completion of the pulse. The model suggested in this work can be extended to describe the first two effects. In order to overcome the difficulty of the third one and to prevent fusion, flushing of the dielectric fluid between the electrodes may help. It is noted that flushing of the dielectric fluid is being considered for control of the voltage across the gap between the electrodes [19].

Acknowledgment

This research work has been sponsored by the Deutschen Forschungs-Gemeinschaft (D.F.G.).

References

1 Williams, E. M., "Theory of Spark Machining," *AIEE Trans.*, Vol. 71, 1952, pp. 105–108.

2 Williams, E. M., Woodford, J. B., and Smith, R. E., "Recent Developments in the Theory and Design of Electric Spark Machining Tools," *AIEE Trans.*, Vol. 73, 1954, pp. 83–88.

3 Williams, E. M., and Smith, R. E., "Phenomena Accompanying Transient Low-Voltage Discharges in Liquid Dielectric (1)," *AIEE Trans.*, Vol. 74, 1955, pp. 164–169.

4 Williams, E. M., and Smith, R. E.," Phenomena Accompanying Transient Low-Voltage Discharges in Liquid Dielectric (2)," *AIEE Trans.*, Vol. 76, 1957, pp. 94–97.

5 Hockenberry, T. O., and Williams, E. M., "Dynamic Evolution of Events Accompanying the Low-Voltage Discharges Employed in EDM," *IEEE Trans.*, Vol. 1, G.A. No. 4, 1967, pp. 301–309.

6 Zingerman, A. S., "The Effect of Thermal Conductivity Upon the Electrical Erosion of Metals, "*Soviet Physics Technical Physics*, Vol. 1, 1957, pp. 1945–1958.

7 Zingerman, A. S., "Electro Erosional Properties of Metals," *Physics of Metals and Metallography*, Vol. 5, 1957, pp. 58–67.

8 Zolotych, B. N., "The Mechanism of Electrical Erosion of Metals in Liquid Dielectric Media," *Soviet Physics Technical Physics*, Vol. 4, 1960, pp. 1370–1373.

9 Nekrashevitch, I. G., and Bakuto, I. A., "Present State of Theoretical Concepts of the Electrical Erosion of Metals," in *Electrospark Machining of Metals*, Krasijuk, B. A., ed., Consultant Bureau, New York, 1965, pp. 17–22.

Downloaded From: https://heattransfer.asmedigitalcollection.asme.org on 06/29/2019 Terms of Use: http://www.asme.org/about-asme/terms-of-use

10 Afanasiev, N. V., "Theory and Calculation of Electric Erosion Process," in *Electrospark Machining of Metals,* Krasijuk, B. A., ed., Consultant Bureau, New York, 1965, pp. 60–66.

11 Saito, N., "Mechanism of Electric Discharge Machining," *Bulletin of the Japanese Society of Proceedings Engineer,* Vol. 1, No. 2, 1964, pp. 95–101.

12 Heuvelman C. J., "Some Aspects of the Research on Electro-Erosion Machining," *Annals of CIRP,* Vol. XVII, 1969, pp. 195–199.

13 Zolotych, B. N., "Theorie zum Phanomen der Funkenerosiven Bearbeitung," *Fertigung,* Vol. 2, 1971, pp. 185–191.

14 Snoeys, R., and Van-Dyck, F., Investigation of Electrodischarge Machining Operations by Means of Thermo Mathematical Model, *Annals of the CIRP,* Vol. 20, 1971, pp. 35–36.

15 Boley, B. A., "The Analysis of Problems of Heat Conduction and Melting," *High Temperature Structure and Materials, Proceedings of 3rd Symposium on Naval Structural Mechanics,* Pergamon Press, Oxford, 1963.

16 Muehlbauer, J. C., and Sunderland, J. E., "Heat Conduction With Freezing or Melting," *Appl. Mech. Rev.,* Vol. 8, 1965, pp. 951–959.

17 Budhia, H., and Kreith, F., "Heat Transfer With Melting or Freezing in a Wedge," *International Journal of Heat and Mass Transfer,* Vol. 16, 1973, pp. 195–211.

18 Sikarskie, D. L., and Boley, B. A., "The Solution of a Class of Two-Dimensional Melting and Solidification Problems," *International Journal of Solids Structures,* Vol. 1, 1965, pp. 207–234.

19 Pedroso, R. I., and Domoto, G. A., "Exact Solution by Perturbation Method for Planar Solidification of Saturated Liquid With Convection at the Wall," *International Journal of Heat and Mass Transfer,* Vol. 16, 1973, pp. 1816–1819.

20 Lazaridis, A., "A Numerical Solution of the Multidimensional Solidification (or Melting) Problem," *International Journal of Heat and Transfer,* Vol. 13, 1970, pp. 1459–1477.

21 Greene, J. E., and Guerrero-Alvarez, J. L., "Electro Erosion of Metal Surfaces,j' *Metallurgical Transactions,* Vol. 5, 1974, pp. 695–706.

22 Crookall, J. R., and Heuvelman, C. J., "Electro-Discharge Machining—the State of the Art," *Annals of the CIRP,* Vol. 20, 1971, pp. 113–120.

23 Cobine, J. D., and Burger, E. E., "Analysis of Electrode Phenomena in the High Current Arc," *J. Appl. Phys.,* Vol. 26, 1955, pp. 895–900.

24 Smithells, C. J., *Metals Reference Book.* Vol. 3, Butterworths, London, Fourth ed., 1967.

25 Nekrashvich, I. G., and Nitkerich, S. P., "Some Relationships of the Phenomena of the Electrical Erosion of Metals in a Low Voltage Discharge in a Liquid," *Soviet Physics Technical Physics,* Vol. 1, 1956, pp. 83–88.

26 Konnerth, K. L., "A Systematic Experimental Study of Electrode Phenomena Accompanying Transient Low Voltage Arcs in Liquid Dialectrics," PhD dissertation, Department of Electrical Engineering, Carnegie Institute of Technology, 1961.

27 Winograd, U., and Almagor, M., "Experimental Investigation of Electric Discharge Machining by Radioactive Tracers," *J. Eng. Materials and Technology,* TRANS. ASME, 1973, pp. 99–102.

28 Carslaw, H. S., and Jaeger, J. C., *Conduction of Heat in Solids.* Oxford, 1959.

Downloaded From: https://heattransfer.asmedigitalcollection.asme.org on 06/29/2019 Terms of Use: http://www.asme.org/about-asme/terms-of-use